

# Phase diagram of a six-state chiral Potts model

H. Meyer<sup>a,1</sup>, J.C. Anglès d'Auriac<sup>a,2</sup>, J-M. Maillard<sup>b,3</sup>,  
G. Rollet<sup>b,4</sup>

<sup>a</sup> *Centre de Recherches sur les Très Basses Températures, BP 166, 38042 Grenoble, France*

<sup>b</sup> *Laboratoire de Physique Théorique et des Hautes Energies, Université de Paris, Tour 16, premier étage, boîte 126, 4 Place Jussieu, F-75252 Paris Cedex 05, France*

Received 11 February 1994

---

## Abstract

We study the phase diagram of an isotropic six-state chiral Potts model on a square lattice by means of both exact and numerical methods. The phase diagram of this model presents many similarities with the phase diagrams of the Ashkin-Teller model or the models studied by Zamolodchikov and Monarstirskii. A remarkable line globally invariant under a transformation generalizing the Kramers-Wannier duality seems to correspond to a first order transition line up to a bifurcation point where this line splits into two second order lines. All the numerical calculations are compared with exact results which can be performed using a canonical elliptic parametrization of this model. The bifurcation point is found to correspond to the intersection of a generalized self-dual line with an algebraic curve. This curve corresponds to the set of points of the phase diagram for which a non-trivial infinite symmetry group of the model degenerates into a finite group of order six. The agreement between numerical and analytical results is very good.

---

## 1. Introduction

For a long time the chiral Potts model was seen as a good toy model to understand important physical issues such as commensurate-incommensurate

---

<sup>1</sup> E-mail: hmeyer@crtbt.polycnrs-gre.fr

<sup>2</sup> E-mail: dauriac@crtbt.polycnrs-gre.fr

<sup>3</sup> E-mail: maillard@lpthe.jussieu.fr

<sup>4</sup> E-mail: rollet@lpthe.jussieu.fr

transitions, floating phases or the occurrence of very rich phase diagrams even for two dimensional systems. The physics emerging from chirality is far to be understood. This interest materialized with the discovery of new solutions of the Yang-Baxter equations for the chiral Potts models [1,2]. These integrability cases happened to be the first genus greater than one solutions of the Yang-Baxter equations [3,4]. In the last years particular efforts have been devoted specifically to the three-state chiral Potts model [5]. Despite its smaller number of parameters, this model already exhibits a rich phase diagram and many subtleties [6].

All the known chiral solutions of the Yang-Baxter equations concern models with cyclic Boltzmann weight matrices. One may ask if any exact result can be obtained for more general nearest neighbor spin models when one does *not* impose this cyclicity condition anymore. From the analysis of the infinite discrete symmetry group generated by inversion relations such a non cyclic, non symmetric six-state model has been proposed <sup>5</sup> [7–9]. This model, when isotropic, depends only on two independent parameters. An explicit elliptic parametrization compatible with the symmetries of the model was given [7,8]. The exact calculation of the partition function using this elliptic foliation remains an open question: this model is not Yang-Baxter integrable, but one may hope getting the partition function using the so-called “inversion trick” together with this parametrization [10–13].

## 2. The model

We study the two dimensional six-state model, denoted  $P_3$  in [7], defined by the following Boltzmann weight matrix:

$$W = \begin{pmatrix} x & y & z & y & z & z \\ z & x & y & z & y & z \\ y & z & x & z & z & y \\ y & z & z & x & z & y \\ z & y & z & y & x & z \\ z & z & y & z & y & x \end{pmatrix} \quad (2.1)$$

Parameters  $x$ ,  $y$  and  $z$  are homogeneous Boltzmann weights. From now on we will use two independent parameters  $u = y/x$  and  $v = z/x$ . This form (2.1) of the matrix  $W$  has a number of remarkable properties. It is invariant under two involutions. The first one is the usual matrix inversion  $I$ , while the second one is the element by element inversion  $J$ . These two transformations  $I$  and  $J$  generate an infinite discrete group of symmetries of the model. The

<sup>5</sup> Inversion relations have been shown to be powerful tools to analyze the phase diagram of lattice models and, in particular, to get the critical manifolds of these models when they are algebraic varieties [10,11,14–19].

Boltzmann matrices can be expressed as  $W(x, y, z) = x\mathbf{1} + yA + zB$ . They belong to a six-dimensional representation of an abelian subalgebra of the algebra of the non-abelian group  $S_3$  of permutations of three elements. We have the following product laws in this subalgebra:

$$A^2 = \mathbf{1} + B, \quad B^2 = 2 + 2A + B, \quad AB = BA = \mathbf{1} + A + B.$$

The group  $S_3$  is known to be the semi-direct product of the groups  $Z_2$  and  $Z_3$ . This suggests that the model could be seen as a non-trivial coupling of an Ising model and of a three-state Potts model. This can directly be seen on the block structure of the  $6 \times 6$  matrix  $W$ . This phenomenological approach needs to be investigated. In particular, the regions of the parameter space where Ising behaviour and three-state Potts model behaviour dominate have to be specified.

Model (2.1) does not show any geometrical “Kramers-Wannier-like duality” [20]. However this duality is replaced by a set of 24 infinite order collineations intertwining the two inversions  $I$  and  $J$ , as the Kramers-Wannier duality does for a usual nearest neighbor interaction spin model [7,8]. The phase diagram of a large number of spin models for which the spins belong to solvable groups (i.e.  $Z_N \propto Z_M$ ) [22] have been analyzed in the literature using extensively the Kramers-Wannier duality [20]. Most of this analysis relies on the prejudice that the lines invariant under this duality are critical, at least on an interval, up to a bifurcation point where it splits into two critical curves. The Ashkin-Teller model can be seen as a paradigm of this situation [12,23,24]. It is tempting, for the six-state chiral Potts model of this paper, to ask if one could have such an “Ashkin-Teller scenario”, the Kramers-Wannier duality being replaced by collineations. The explicit elliptic parametrization can also help to answer this question.

### 3. Exact results

Introducing for this model the variables  $u = y/x$ ,  $v = z/x$ , the explicit formulae for the inversion  $I$  are

$$I : (u, v) \longrightarrow \left( \frac{-u^2 - u + 2v^2}{1 + u + 2v - u^2 - 2uv - v^2}, \frac{u^2 + vu - v^2 - v}{1 + u + 2v - u^2 - 2uv - v^2} \right), \tag{3.1}$$

and the involution  $J$  reads

$$J : (u, v) \longrightarrow \left( \frac{1}{u}, \frac{1}{v} \right). \tag{3.2}$$

The two involutions  $I$  and  $J$  generate an infinite discrete group of birational transformations [7–9]. Noticeably the algebraic expression

$$\Delta(u, v) = \frac{(2v^2 + 2vu - u^2 - 2u^3 - 2vu^2 + v^2u)(u - v^2)^2}{(v + u)^4(1 - u)(1 - v)^2} \tag{3.3}$$

is invariant under this infinite set of birational transformations. The curves  $\Delta(u, v) = \delta$ , where  $\delta$  is some constant, are all elliptic curves. Two remarkable situations occur: for a finite number of values of the constant  $\delta$  the elliptic curve degenerates into rational curves [7,9] and for an infinite number of values of  $\delta$  the curve  $\Delta(u, v) = \delta$  corresponds to points for which the previous group generated by  $I$  and  $J$  degenerates into a *finite order* group (details are given in [7–9]). Among these values of  $\delta$ , two are of special interest for this paper. Firstly,  $\delta = 3/16$  corresponds to the standard Potts line  $u = v$  for which one can introduce a rational parametrization together with a curve of higher degree that we will not write here. Secondly,  $\delta = 0$  corresponds to two branches:  $u = v^2$ , for which  $(IJ)^3(u, v) = (u, v)$  and which is obviously a rational curve, and the curve given by the equation

$$2v^2 + 2vu - u^2 - 2u^3 - 2vu^2 + v^2u = 0 \tag{3.4}$$

for which  $(IJ)^6(u, v) = (u, v)$ . Remarkably this last curve is also a *rational* curve [25]. Let us give here a rational parametrization of this curve:

$$u = \frac{2 + 2t - t^2}{2t^2 + 2t - 1}, \quad v = \frac{2 + 2t - t^2}{t \cdot (2t^2 + 2t - 1)}. \tag{3.5}$$

Conversely, eliminating  $t$  in (3.5), one gets back *only* to (3.4). Using this rational parametrization the two involutions  $I$  and  $J$  take the very simple form:

$$I : t \rightarrow \frac{2 + t}{t - 1}, \quad J : t \rightarrow \frac{1}{t}, \tag{3.6}$$

and an infinite generator  $J I$  reads:

$$J I : t \rightarrow \frac{t - 1}{2 + t}.$$

It is then suitable to introduce the variable  $x$  :

$$x = \frac{t + 1/r}{t + r},$$

where  $r = \frac{1}{2} + i \cdot \frac{\sqrt{3}}{2}$  is a sixth root of unity. In terms of the well-suited variable  $x$  and the sixth root  $r$ , transformations  $I$  and  $J$  take a simple multiplicative form:

$$I : x \rightarrow \frac{1}{rx}, \quad J : x \rightarrow \frac{1}{r^2x}. \tag{3.7}$$

Let us also recall that the standard six-state Potts line  $u = v$  ( $\delta = 3/16$ ) has a ferromagnetic first order transition point localized at  $u = v = 1/(1 + \sqrt{6})$  [12].

On another hand, when a Kramers-Wannier duality exists on an edge spin model, it is possible to show that this duality, denoted  $D$ , actually intertwins  $I$  and  $J$  (i.e.  $I = D^{-1} \cdot J \cdot D$ ),  $D$  being an involution or a transformation of order four [4]. In the case of the chiral Potts model studied here, it is not possible to find such a geometrical “Kramers-Wannier-like duality”. However  $I$  and  $J$  being two birational involutions of two variables, a theorem by Noether [27] states <sup>6</sup> that  $I$  can be expressed as a product of collineations and  $J$ . Actually there exists a set of collineations  $C_i$  intertwining the two involutions  $I$  and  $J$  ( $I = C_i^{-1} \cdot J \cdot C_i$ ). This situation generalizes the one encountered with standard dualities. It turns out that there are 24 such collineations, but the collineation

$$C_0 : (u, v) \rightarrow \left( \frac{1 - u}{1 + 2u + 3v}, \frac{1 - v}{1 + 2u + 3v} \right)$$

plays a special role. Indeed all the 24 collineations  $C_i$  can be deduced from  $C_0$  using 24 different collineations  $X_{i,0}$  as follows:

$$C_i = X_{i,0} \cdot C_0 .$$

The  $X_{i,0}$ ’s commute with  $J$  ( $X_{i,0} \cdot J = J \cdot X_{i,0}$ ) and form a group of 24 elements (the  $C_i$  do *not* form a group). This group is isomorphic to the semi-direct product of  $S_3$  with  $Z_2 \times Z_2$ . A complete list of these collineations  $C_i$  and  $X_{i,0}$ , as well as a detailed analysis of the structure of this 24 element group, will be given elsewhere. It is important to note that none of the 24 collineations  $C_i$  is of *finite* order. However, in the standard Potts limit ( $u = v$ ) the collineation  $C_0$  reduces to the known involutive duality transformation [20,21,28]:

$$u \rightarrow \frac{1 - u}{1 + 5u} .$$

Thus  $C_0$  can be seen as a generalization of the standard duality transformation. The lines *globally* invariant under  $C_0$  are the standard Potts line  $u = v$  together with the line  $2u + 3v + A = 0$  where  $A$  is one of the roots of the quadratic polynomial  $5 + 2A - A^2 = 0$ . The line corresponding to the negative root ( $A = -1.449489743$ ) is:

$$2u + 3v = \sqrt{6} - 1 . \tag{3.8}$$

It has an interval belonging to the ferromagnetic physical region of the parameter space and intersects the standard Potts model line  $u = v$  at the first order

<sup>6</sup> In  $CP_2$ , the Noether theorem proves that every birational automorphism of the plane can be represented as a product of quadratic transformations and a projective transformation. This is very specific to  $CP_2$ , the birational transformations in  $CP_n$ ,  $n > 2$ , are much more complicated.

transition point. Thus this line, which is invariant under a generalized duality transformation, can be seen as a generalized self-dual line. Moreover it can be shown (detailed calculations will be given elsewhere) that an argument due to Kardar [26] can be generalized to the Potts model studied here. This argument shows that the ferromagnetic first order transition point of the standard Potts model is not an isolated transition point. It also shows that the critical curve passing by this point has the same slope as line (3.8), and that the transition in the neighborhood of the ferromagnetic point of the standard model is first order.

Finally it is worth noting that line (3.8) intersects curve (3.4) at a point  $B$  where the symmetry group degenerates into a finite group of order 6. It is likely that point  $B$  is a point of enhanced symmetry and plays a special role in the phase diagram. The location of this point can easily be found using parametrization (3.5). The value of  $t$  corresponding to the point  $B$  is one of the roots of

$$24t^6 + 48t^5 - 9t^4 - 78t^3 - 111t^2 - 108t - 36 = 0.$$

Using the correct root  $t_B = 1.580846966$  one finds the location of point  $B$ :

$$(u_B, v_B) = (0.3718817401, 0.2352420875). \quad (3.9)$$

#### 4. The phase diagram

In order to determine the phase diagram in the ferromagnetic region of the model defined by the Boltzmann weight matrix (2.1) we have performed extensive Monte Carlo simulations. We always worked on a square lattice with periodic boundary conditions. We found it convenient for numerical calculations to use the following parametrization of the  $(u, v)$ -plane:

$$u = \exp\left(\frac{-\rho}{T}\right), \quad v = \exp\left(\frac{-1}{T}\right).$$

The square  $0 \leq u, v < 1$  ( $\rho > 0$ ) is the ferromagnetic region where the ground-state is ordered with one single color. The value  $\rho = 1$  corresponds to the standard six-state Potts model. In the phase diagram on Fig. 1 some iso- $\rho$  curves are presented. On these curves the energy is well defined as a function of temperature ( $J_x = 0$ ,  $J_y = -\rho$ ,  $J_z = -1$ ); this enables us to use different criteria to check equilibrium. Using the fluctuation-dissipation theorem it is straightforward to relate the fluctuation of the energy per spin and a numerical derivative of this energy with respect to the temperature: we systematically discarded all our results where this relation was not verified with a good accuracy and kept only those for which the complete energy distribution  $P(E)$  was reliable. From this distribution at a given temperature

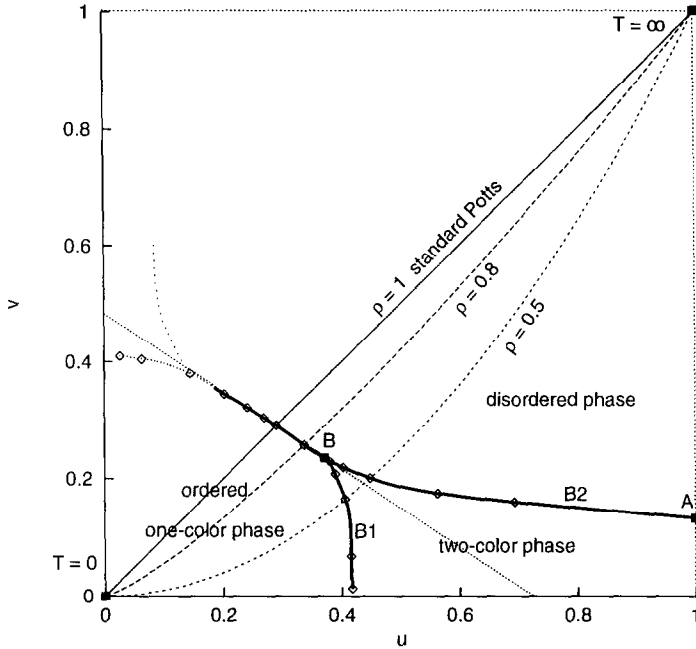


Fig. 1. Ferromagnetic region of the phase diagram in variables  $u$  and  $v$ . Iso- $\rho$  lines for  $\rho = 1$ ,  $\rho = 0.8$  and  $\rho = 0.5$  are presented.

and a given asymmetry  $\rho$ , we are able to extrapolate the energy distribution in the neighborhood of a point of simulation using the histogram method in two dimensions [29,30] adapted to our case. Comparison of extrapolations from different simulation points provides another independent test of equilibrium. When error bars are drawn on a figure they are calculated as the mean square deviation of the average of fifty independent measurements. The sizes analyzed in this work are  $L = 32$ ,  $L = 64$  and  $L = 128$ . All calculations were performed on a parallel computer of twelve i860 processors. Altogether it represents  $3 \times 10^{12}$  updates.

We first checked the whole procedure on the standard Potts model ( $\rho = 1$ ) for which many quantities are exactly known at the transition point in the thermodynamical limit [12,28]. It provides a comparison for other values of  $\rho$ . For  $\rho = 0.8$  we found a very similar behaviour, locating a first order transition very close to the line (3.8). Fig. 2 shows the energy distribution at the transition point and at a different temperature slightly below the transition. The bimodal form of this distribution leaves no doubt about the first order character of the transition.

The situation is very different for a value of the asymmetry like  $\rho = 0.5$ . Fig. 3 presents the specific heat for different values of  $L$  deduced from the fluctuations. The points are the results of the simulation, and the lines are obtained by extrapolation using the histogram method [29]. The presence of

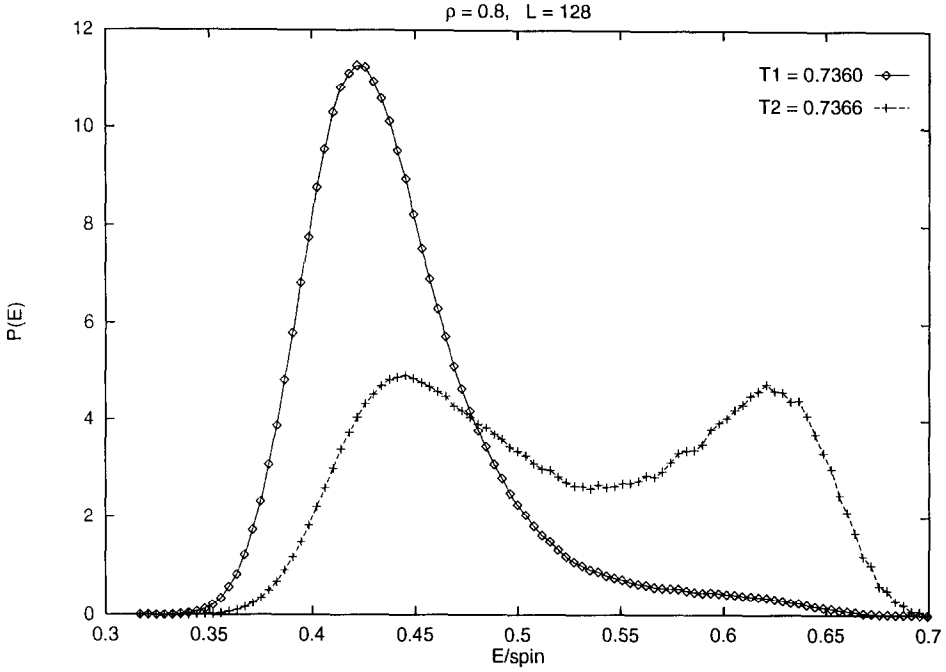


Fig. 2. Probability distribution  $P(E)$  of energy  $E$  for  $\rho = 0.8$  on a square lattice of linear size  $L = 128$ . The curve for  $T_1 = 0.736$  is the result of a simulation. The other curve for  $T_2 = 0.7366$  was obtained transforming the first one.

two maxima is clear. The size behaviour of the amplitude of these maxima indicates two transitions. It is then necessary to determine what are the order parameters for these two transitions. The form of the Boltzmann matrix (2.1) together with the fact that  $u > v$  suggest to define the two following order parameters  $m_1$  and  $m_2$ :

$$m_1 = \frac{1}{L^2} \sum_i \left| (\delta_{\sigma_i,0} + \delta_{\sigma_i,1} + \delta_{\sigma_i,2}) - (\delta_{\sigma_i,3} + \delta_{\sigma_i,4} + \delta_{\sigma_i,5}) \right|, \tag{4.1}$$

$$m_2 = \frac{1}{L^2} \sum_i \left| (\delta_{\sigma_i,0} + \delta_{\sigma_i,3}) - (\delta_{\sigma_i,2} + \delta_{\sigma_i,5}) \right|. \tag{4.2}$$

Parameter  $m_1$  amounts to identify colors 0, 1 and 2 and colors 3, 4 and 5. Parameter  $m_2$  amounts to identify colors with a difference of 3. The intuitive idea behind these two parameters is the following. At high temperature the system is invariant under permutation of arbitrary colors, this is a paramagnetic phase. For intermediate temperature the full symmetry is broken and only the exchange of two colors of difference three (0-3, 1-4 or 2-5) leaves the system invariant, this is a two-color phase. Eventually for low temperature one recovers a ferromagnetic phase with one dominating color. Fig. 4 presents the

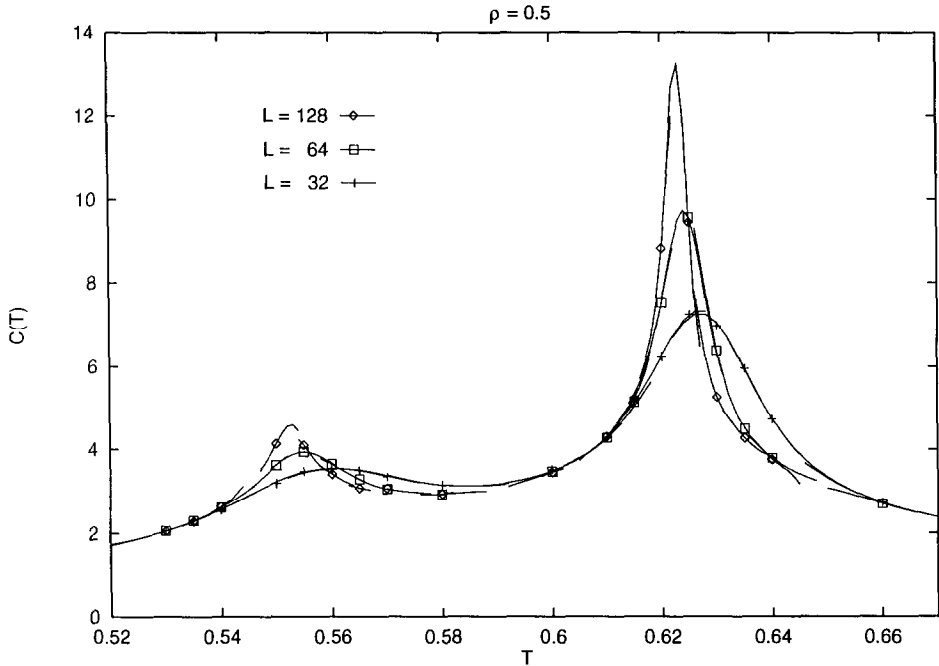


Fig. 3. Specific heat  $c_v(T)$  as a function of the temperature  $T$  for different sizes  $L = 32$ ,  $L = 64$  and  $L = 128$  and for  $\rho = 0.5$ . The points are results of the simulation, and the lines are obtained by extrapolation using the histogram method.

two parameters  $m_1$  and  $m_2$  for  $\rho = 0.5$  as functions of the temperature  $T$  for  $L = 64$ . The order parameter behaviour is clearly seen and the temperatures for which these parameters almost vanish coincide with the two maxima of the specific heat. We then performed finite size scaling analysis to determine the universality class of these two second order phase transitions. The results are summarized in Fig 5. Fig. 5(a) shows the raw data i.e. parameter  $m_1$  as a function of the temperature  $T$  for different values of  $L$ . Fig. 5(b) presents the same data using the reduced variables  $y = m(T) \cdot L^{\beta/\nu}$  and  $x = (T - T_c) \cdot L^{1/\nu}$ . The best fit is obtained for the values  $\beta = 0.12$ ,  $\nu = 1$  and  $T_c = 0.553$ . Our data for  $\rho = 0.5$  are thus compatible with a second order phase transition of the Ising type ( $\beta = 1/8$  and  $\nu = 1$ ). The question to know if the critical exponents are fixed along this lower branch  $B_1$  will be addressed in a forthcoming publication. Moreover we want to determine the universality class of the upper branch  $B_2$  that one could expect to be that of the three-state standard Potts universality class ( $\beta = 1/9$  and  $\nu = 5/6$ ).

We performed other simulations for intermediary values of  $\rho$  in order to understand the region between  $\rho = 0.8$ , for which one has a first order transition, and  $\rho = 0.5$ , for which two second order transitions occur. We used different methods to locate precisely the “bifurcation” point  $B$  where the first

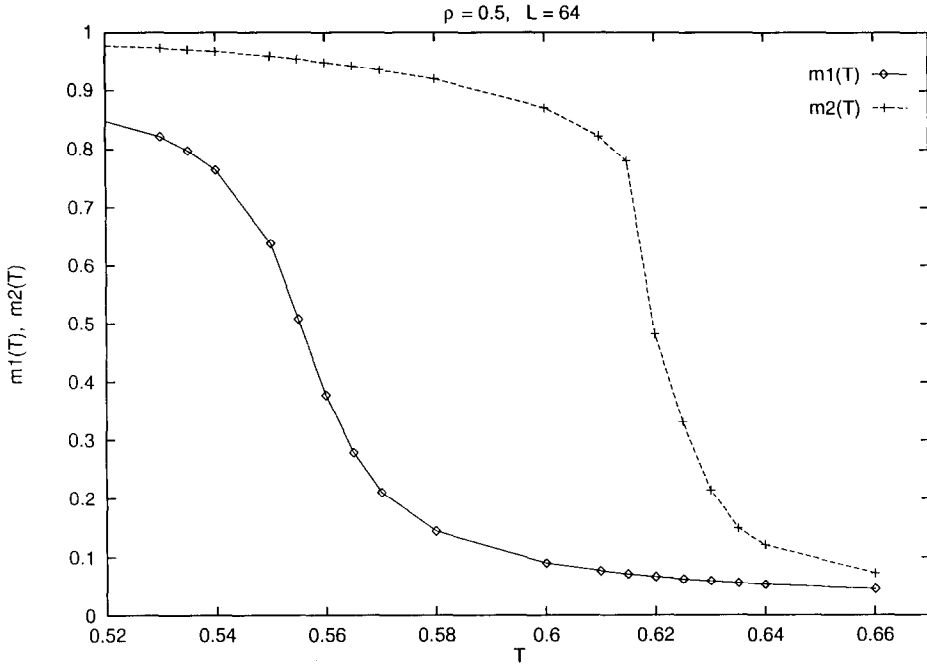


Fig. 4. The two order parameters  $m_1(T)$  and  $m_2(T)$  as a function of the temperature  $T$  for  $L = 64$  and for  $\rho = 0.5$ . The lines are a guide to the eye.

order transition line splits into two second order critical lines  $B_1$  and  $B_2$ . The most simple one was to consider the number of maxima of the specific heat for different values of  $\rho$ . The presence of two maxima indicates two transitions, while a single maximum indicates only one transition. To address the question of the order of the transition, we considered the probability distribution of the internal energy per spin for different values of  $\rho$  and at the temperature where the maxima occur. Fig. 6 shows these distributions for  $\rho = 0.66$  and  $T = 0.6810$ , for  $\rho = 0.70$  and  $T = 0.6967$ , for  $\rho = 0.74$  and  $T = 0.7132$  and finally for  $\rho = 0.80$  and  $T = 0.7372$  on a lattice of linear size  $L = 64$ . These distributions are obtained by transforming the histogram with respect to temperature, keeping the asymmetry  $\rho$  constant. Eventually we used a more refined technique. We measured the fluctuations of the three quantities  $n_x$ ,  $n_y$  and  $n_z$  which are the numbers of bonds with Boltzmann weight  $x$ ,  $y$  and  $z$  (see (2.1)). For the standard Potts model the fluctuations of these three quantities  $n_x$ ,  $n_y$  and  $n_z$  are proportional and exhibit a sharp maximum at the same temperature. We recovered this behaviour when we have a single transition. On the other hand, for example for  $\rho = 0.5$ , the fluctuations of  $n_y$  are maximum at the lowest critical point  $T_{c1}$ , while the fluctuations of  $n_z$  are only maximum at the higher transition  $T_{c2}$ . The coincidence of these maxima of the fluctuations of  $n_x$ ,  $n_y$  or  $n_z$  give a criterion to locate the bifurcation point

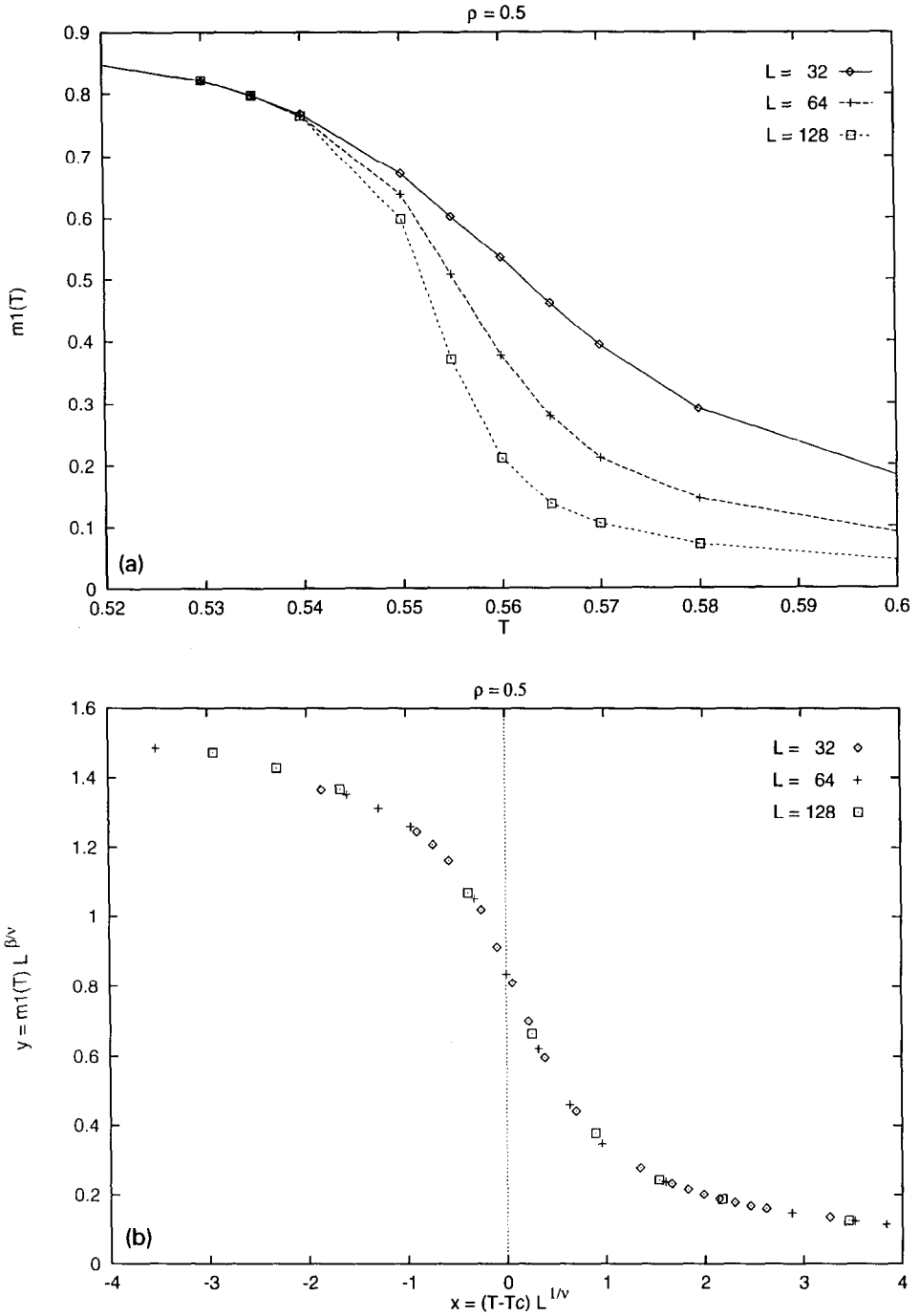


Fig. 5. (a) Parameter  $m_1(T)$  for  $\rho = 0.5$  as a function of  $T$  for  $L = 32$ ,  $L = 64$  and  $L = 128$  (raw data). (b) Same data using reduced variables  $x$  and  $y$  with  $\beta = 0.12$ ,  $\nu = 1$  (see text).

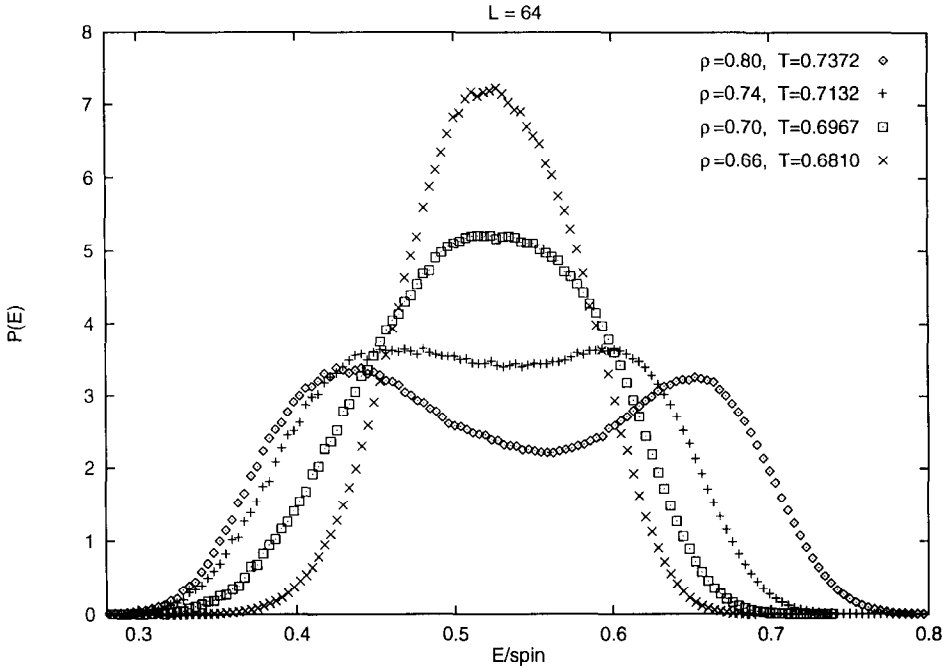


Fig. 6. Probability distributions  $P(E)$  of energy  $E$  for  $L = 64$  near transition temperature. The four distributions correspond to  $\rho = 0.66$  and  $T = 0.6810$ ,  $\rho = 0.70$  and  $T = 0.6967$ ,  $\rho = 0.74$  and  $T = 0.7132$  and  $\rho = 0.80$  and  $T = 0.7372$ .

*B.* Using these methods we found  $\rho = 0.68$  and  $T = 0.69$  giving  $u = 0.373$  and  $v = 0.235$ . This is in good agreement with the exact prediction (3.9).

To complete the phase diagram, we also performed Monte Carlo simulations for other values of  $\rho$ . We paid special attention to  $\rho = 0$  ( $u = 1$ ). In this case the ground-state is not of standard ferromagnetic type anymore. Instead it consists of two colors of difference three in complete disorder. Thus the ground-state has a non zero residual entropy per spin. These ground-states are of two-color type. Therefore we expect a single transition point located on the upper branch  $B_2$ . Indeed, we found for  $\rho = 0$  a second order phase transition point, thus locating the point  $A$  where the upper branch  $B_2$  intersects the frontier of the ferromagnetic region with a “semi-ferromagnetic” region ( $u > 1$ ,  $v < 1$ ). The coordinates of this point are  $u_A = 1$ ,  $v_A = 0.133$ . All these results are summarized in Fig. 1 which shows the proposed phase diagram for this model.

## 5. Summary and speculations

We proposed a phase diagram for a six-state chiral Potts model. This phase diagram is reminiscent of the Ashkin-Teller model scenario. A line globally invariant under a transformation generalizing the duality is a first order critical line up to a bifurcation point  $B$  where it splits in two second order branches. The lower branch, at least near  $\rho = 0.5$  is compatible with the Ising universality class. Some questions remain to be confirmed and will be addressed in forthcoming publications. We want to confirm that the two branches  $B_1$  and  $B_2$  have *fixed* critical exponents of the Ising and  $q = 3$  universality class. Keeping in mind the Ashkin-Teller scenario [24] one may have the prejudice that another bifurcation point occurs in the  $v \geq u$  part of the ferromagnetic region of the parameter space. A good candidate for such a bifurcation point is the intersection of line (3.8) together with the curve  $u = v^2$  for which the symmetry of the model is modified. Preliminary results seem in good agreement with this hypothesis. Finally one would like to sketch the analysis of the two “semi-antiferromagnetic” phases  $u \geq 1, v \leq 1$  and  $u \leq 1, v \geq 1$  as well as the antiferromagnetic region.

## Acknowledgement

This work has been supported by CNRS. We thank M.P. Bellon and C.M. Viallet for stimulating discussions.

## References

- [1] H. Au-Yang, B.M. Mc Coy, J.H.H. Perk, S. Tang and M.L. Yan, Phys. Lett. A 123 (1987) 219.
- [2] B.M. Mc Coy, J.H. Perk, S. Tang and C.H. Sah, Phys. Lett. A 125 (1987) 9.
- [3] R.J. Baxter, J.H.H. Perk and H. Au-Yang, Phys. Lett. A 128 (1988) 138.
- [4] D. Hansel and J.M. Maillard, Phys. Lett. A 133 (1988) 11.
- [5] R.J. Baxter, J. Stat. Phys. 70 (1993) 535.
- [6] J.C. Anglès d’Auriac, D. Hansel and J.M. Maillard, J. Phys. A 22 (1989) 2577.
- [7] M.P. Bellon, J-M. Maillard and C-M. Viallet, Phys. Lett. A 159 (1991) 221.
- [8] M.P. Bellon, J-M. Maillard and C-M. Viallet, Phys. Lett. A 159 (1991) 233.
- [9] M.P. Bellon, J-M. Maillard and C-M. Viallet, Phys. Rev. Lett. 67 (1991) 1373.
- [10] J.M. Maillard, J. Math. Phys. 27 (1986) 2776.
- [11] R.J. Baxter, in: Proc. of the 1980 Enschede Summer School: Fundamental Problems in Statistical Mechanics, vol. V (North-Holland, Amsterdam, 1981).
- [12] R.J. Baxter, Exactly Solved Models in Statistical Mechanics (Academic Press, London, 1982).
- [13] J.M. Maillard, J. de Physique 46 (1984) 329.
- [14] J.M. Maillard and R. Rammal, J. Phys. A 16 (1983) 353.
- [15] M.T. Jaekel and J.M. Maillard, J. Phys. A 15 (1982) 2241.
- [16] R.J. Baxter, J. Stat. Phys. 28 (1982) 1.
- [17] Y.G. Stroganov, Phys. Lett. A 74 (1979) 116.
- [18] J.M. Maillard, in: Brasov International Summer School on Critical Phenomena, Theoretical Aspects (Birkhäuser, 1983).

- [19] D. Hansel, J.M. Maillard and P. Rujan, *Int. J. Mod. Phys. B* 3 (1989) 1539.
- [20] N.L. Biggs, *Math. Proc. Cambr. Philos. Soc.* 80 (1976) 429.
- [21] N.L. Biggs, *Interaction Models, Lecture Notes Series 30* (Cambridge University Press, 1977).
- [22] A.B. Zamolodchikov and M.I. Monastyrskii, *Sov. Phys. J.E.T.P.* 50 (1979) 167.
- [23] J. M. Maillard and P. Rujan and T. Truong, *J. Phys. A* 18 (1985) 339.
- [24] R.V. Ditzian et al., *Phys. Rev. B* 22 (1980) 2542.
- [25] M.P. Bellon, J-M. Maillard and C-M. Viallet, *Phys. Lett. A* 157 (1991) 343.
- [26] M. Kardar, *Phys. Rev. B* 26 (1982) 2693.
- [27] I.R. Shafarevich, *Basic Algebraic Geometry, Springer Study* (Springer, Berlin 1977), p. 216.
- [28] F.Y. Wu, *Rev. Mod. Phys.* 54 (1982) 235.
- [29] A.M. Ferrenberg and R.H. Swendsen, *Phys. Rev. Lett.* 61 (1988) 2635.
- [30] K. Binder (ed.) *The Monte Carlo Method in Condensed Matter Physics, Topics in Applied Physics*, vol. 71 (Springer Verlag, 1992).